JZUS

Modeling of mass transfer characteristics of bubble column reactor with surfactant present

ZHAO Wei-rong (赵伟荣)[†], SHI Hui-xiang (史惠祥), WANG Da-hui (汪大翚)

(*Department of Environmental Engineering, Zhejiang University, Hangzhou 310027, China*)

[†]E-mail: weirong@mail.hz.zj.cn

Abstract: Danckwert's method was used to determine the specific interfacial area, a, and the individual mass transfer coefficient, k_L, during absorption of CO_2 in a bubble column with an anionic surfactant in the carbonate-bicarbonate buffer solution and $NaAsO_2$ as catalyst, the presence of which decreases the specific interfacial area and the individual mass transfer coefficient. The specific interfacial area and the individual mass transfer coefficient increase with increasing superficial gas velocity. The specific interfacial area decreases whereas the individual mass transfer coefficient increases with increasing temperature. The results of experiments were used to determine the dependence of a, k_L, and $k_L a$ on the surface tension, the temperature of the absorption phase, and the superficial velocity of the gas. The calculated results from the correlation were found to be within 10% deviation from the actual experimental results.

INTRODUCTION

Bubble columns are widely used in the chemical industry where heterogeneous gas-liquid or gas-solid reactions take place, particularly, in which the liquid phase controls mass transfer processes due to the relative insolubility of gases (Vázquez *et al.*, 2000; Lye and Stuckey, 2001). Important applications of bubble columns include oxidation, hydrogenation, ozonolysis, alkylation, column flotation, wastewater treatment, etc. (Yang *et al.*, 2001; Wu *et al.*, 2002).

The design parameters for bubble columns are: gas-liquid specific interfacial area, a, individual mass transfer coefficient, k_L, flow regime, bubble size distribution, and coalescence of bubbles. Most studies on bubble columns were devoted to the experimental determination of some of these parameters, and more specifically, of the volumetric

mass transfer coefficient, $k_L a$, which depends fundamentally on the superficial gas velocity and on the physical properties of the absorption phase. Numerous correlations have been proposed for the superficial velocity of the gas as well as for the viscosity of the liquid phase (Joshi, 2001; Mitsuharu *et al.*, 2001), but correlations for the surface tension of the liquid phase are seldom investigated.

The most frequently used chemical method for determining k_L and a is the Danckwerts method (Vázquez *et al.*, 2000; Cents *et al.*, 2001) based on the absorption of CO_2 in carbonate-bicarbonate buffer solutions. The major advantage of this chemical absorption method over a physical absorption technique is that, when the reaction is fast enough, the bulk concentration of the dissolved gas is negligible which simplifies the determination of driving force for mass transfer calculation (Cents *et al.*, 2001). As a result, it allows for determination of the

mass transfer parameters of k_L and a to be accurate during stationary conditions.

In this paper, k_L and a were determined (by Danckwerts method) from a system of CO_2 absorbed by Na_2CO_3-$NaHCO_3$ (0.5-0.5 mol/L) buffer solution with $NaAsO_2$ as catalyst, and an anionic surfactant, dodecyl benezene sulfonic acid sodium (DBS), as surface tension modifier. The k_L, a, and k_La were then correlated to a function of temperature, superficial gas velocity, and surface tension of the liquid phase.

THEORY

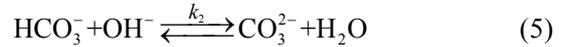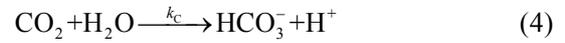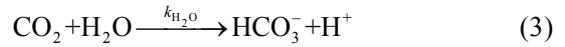The chemical method proposed by Danckwerts (Vázquez *et al.*, 2000; Cents *et al.*, 2001) used to calculate k_L and a requires that the gas absorbed undergoes a moderately fast pseudo-first-order reaction with some of the solutes in the liquid phase. Under these conditions, the absorption rate is given by:

$$N = C_d^e a\sqrt{k_L^2 + k_1 D_d} \qquad (1)$$

with N being the absorption rate per unit volume (mol/L·s); a the specific interfacial area (m^{-1}); C_d^e the gas solubility in solution (mol/L); D_d the gas diffusivity in solution (m^2/s); k_L the individual mass transfer coefficient (m/s); and k_1 the rate-constant of the pseudo-first-order reaction (s^{-1}).

Eq.(1) shows that by changing the value of k_1 a straight line can be obtained by plotting $(N/C_d^e)^2$ versus $k_1 D_d$. In this plot the slope equals to a^2 and $(k_La)^2$ equals the intercept with the vertical axis. In this way k_L and a can be determined simultaneously.

The catalytic absorption of carbon dioxide by alkali carbonates solution occurs as follows:

$$CO_2 + OH^- \xrightarrow{k_{OH^-}} HCO_3^- \qquad (2)$$

$$CO_2 + H_2O \xrightarrow{k_{H_2O}} HCO_3^- + H^+ \qquad (3)$$

$$CO_2 + H_2O \xrightarrow{k_C} HCO_3^- + H^+ \qquad (4)$$

$$HCO_3^- + OH^- \xleftrightarrow{k_2} CO_3^{2-} + H_2O \qquad (5)$$

$$H^+ + OH^- \xleftrightarrow{k_w} H_2O \qquad (6)$$

Eq.(2) is a second-order reaction wherein rate-constant k_{OH^-} (L/mol·s) variation with temperature, T (K), and ionic strength, I (mol/L), being calculated as (Hikita *et al.*, 1976; Vázquez *et al.*, 2000):

$$\lg k_{OH^-} = \lg k_{OH^-}^\circ + 0.20I - 0.0182I^2 \qquad (7)$$

$$\lg k_{OH^-}^\circ = 13.635 - \frac{2985}{T} \qquad (8)$$

The first-order rate-constant of Eq.(3), k_{H_2O} (s^{-1}), can be calculated as:

$$\lg k_{H_2O} = 329.80 - 110.54\lg T - \frac{17265}{T} \qquad (9)$$

The rate-constant of catalytic Eq.(4) at various temperatures, k_C (L/mol·s), can be calculated by the Nernst equation taking activation energy as 47.4 kJ/mol (Danckwerts, 1970) and rate-constant as 350 L/mol·s at 298.15 K (Cents *et al.*, 2001). The results are listed in Table 1.

The equilibrium constant of Eq.(5), k_2 (L/mol), can be calculated as (Hikita *et al.*, 1976; Vázquez *et al.*, 2000; Cents *et al.*, 2001):

$$\lg k_2 = \lg k_2^\circ + \frac{1.01\sqrt{[Na^+]}}{1 + 1.27\sqrt{[Na^+]}} + 0.125[Na^+] \qquad (10)$$

Table 1 Calculation of k_0 and k_C

T (K)	$k_{H_2O} \times 10^3$ (s^{-1})	$k_{OH^-} \times 10^{-3}$ (L/mol·s)	$C_{OH^-} \times 10^5$ (mol/L)	$k_{OH^-} \times C_{OH^-}$ (s^{-1})	k_0 (s^{-1})	k_C (L/mol·s)
288.15	9.9	8.2	1.3	0.107	0.117	251
298.15	23.0	18.0	2.3	0.414	0.437	350
308.15	46.0	37.0	3.8	1.406	1.452	478
318.15	78.0	73.0	6.7	4.891	4.969	640

$$\lg k_2^\circ = \frac{1568.94}{T} + 0.4134 - 0.006737T \qquad (11)$$

and, the equilibrium concentration of hydroxyl ion, $[OH^-]$ (mol/L), can be calculated as:

$$[OH^-] = \frac{[CO_3^{2-}]}{k_2[HCO_3^-]} \qquad (12)$$

Under certain conditions, the absorption of CO_2 by carbonate-bicarbonate buffer solution catalyzed by sodium arsenite can be considered as pseudo-first-order reaction with rate-constant k_1 (s^{-1}). The global reaction is:

$$CO_2 + CO_3^{2-} + H_2O \xrightarrow{k_1} 2HCO_3^- \qquad (13)$$
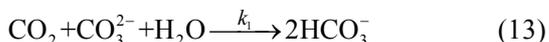
For Eq.(13) to be pseudo-first-order, it is necessary that the concentrations of CO_3^{2-}, HCO_3^-, and OH^- ion must keep constant, without decreasing from the liquid bulk to the interface. Therefore, the following condition must be fulfilled (Vázquez et al., 2000; Cents et al., 2001):

$$C_d^e \left[\frac{1}{[CO_3^{2-}]} + \frac{2}{[HCO_3^-]} \right] \left[\sqrt{1 + \frac{D_d k_1}{k_L^2}} - 1 \right] \ll 1 \quad (14)$$

Under the experimental conditions, the maximum value of left-hand term of Eq.(14) is 0.022 taking the relevant data from Tables 1–4, shown the criterion of Eq.(14) is well satisfied in the experiments.

According to Eqs.(2)–(4), the rate-constant of Eq.(13), k_1, is given by:

$$k_1 = k_{H_2O} + k_{OH^-}[OH^-] + k_C[Cat] = k_0 + k_C[Cat] \quad (15)$$

where k_0 (s^{-1}) and k_C (L/mol·s) are the contributions

Table 2 Diffusivities of carbon dioxide in absorption Phase

T (K)	$D_W \times 10^9$ (m²/s)	$D_d \times 10^9$ (m²/s)
288.15	1.48	1.19
298.15	1.96	1.58
308.15	2.51	2.02
318.15	3.12	2.51

Table 3 Solubilities of CO₂ in absorption phase

T (K)	$(K_s I)_{Na_2CO_3}$	$(K_s I)_{NaHCO_3}$	C^e (mol/L)	$\sum_{i=1}^{2}(K_{si}I_i)$	C_d^e (mol/L)
288.15	0.202	0.094	0.0455	0.296	0.023
298.15	0.194	0.091	0.0339	0.285	0.018
308.15	0.189	0.089	0.0266	0.278	0.014
318.15	0.185	0.088	0.0214	0.273	0.011

Table 4 Summary of experimental results using Danckwerts plots and the calculations of Eqs.(20)–(22)

T (K)	$u_G \times 10^3$ (m/s)	[DBS] (mg/L)	$\sigma \times 10^3$ (N/m)	$k_L \times 10^5$ (m/s)		a (m⁻¹)		$k_L a \times 10^3$ (s⁻¹)	
				Experimental data	Calculation from Eq.(20)	Experimental data	Calculation from Eq.(21)	Experimental data	Calculation from Eq.(22)
288.15	3.1	0	75.03	8.62	9.17	110.2	105.1	9.50	9.64
298.15	3.1	0	75.03	12.81	12.40	105.1	101.5	13.46	12.59
308.15	3.1	0	75.03	15.75	16.44	100.7	98.4	15.87	16.17
318.15	3.1	0	75.03	20.92	21.41	96.6	95.5	20.21	20.44
298.15	2.1	0	75.03	10.77	10.57	72.3	79.3	7.79	8.38
298.15	1.3	0	75.03	8.45	8.68	60.8	58.5	5.14	5.08
298.15	3.1	0.5	72.80	12.40	12.11	102.3	101.6	12.69	12.29
298.15	3.1	1.0	70.54	11.80	11.81	99.6	101.6	11.75	11.99
298.15	3.1	2.0	68.10	11.12	11.48	98.3	101.6	10.93	11.66
298.15	3.1	5.0	64.73	10.89	11.02	97.3	101.6	10.59	11.20

of the non-catalyzed and catalyzed reaction, respectively; and [Cat] represents the concentration of the catalyst, i.e. the concentration of the arsenite ion.

Under the experimental conditions, k_0 can be calculated through Eqs.(7)–(12). The results are listed in Table 1.

As shown in Table 1, the advantage of this method is that the appreciable differences of k_1 can be obtained using very small catalyst concentrations, thereby, not affecting the physical properties of the absorption phase.

MATERIALS AND METHODS

Mass transfer measurements

Mass transfer measurements were carried out using the apparatus shown in Fig.1.
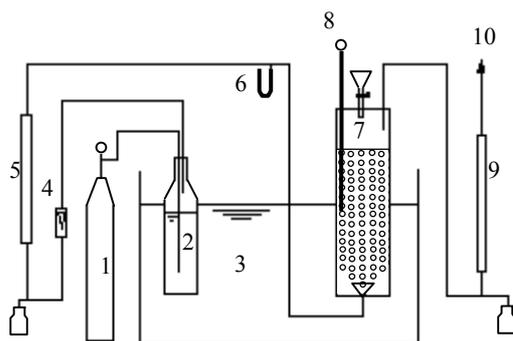
Fig.1 Schematic diagram for experimental set-up
1: carbon dioxide; 2: humidifier; 3: thermostat; 4: flowmeter; 5, 9: soap-film meter; 6: barometer; 7: bubble column reactor; 8: thermometer; 10: gas out

A bubble column with height of 60 cm (7) was used as the contact device, made of glass cylindrical tube, sealed with rubber cap and o-ring. The internal and external diameters of the column are 10.2 cm and 10.8 cm, respectively.

The absorption phases used (0.5-0.5 mol/L sodium carbonate-bicarbonate buffer solutions with sodium arsenite as catalyst, and DBS as surface tension modifier) were thermostated before CO_2 gas was introduced into the contact device. For each batch run, the liquid load was 3.5 L. The concentration ranged from 0 to 0.008 mol/L for sodium arsenite, and from 0 to 5 mg/L for DBS.

The pure CO_2 gas (1) to be absorbed was passed through a humidifier (2) and then entered the contact device (7) at a constant flow rate measured with a soap-film meter (5). Gas outflow through the outflow port in the top-plate was measured with another soap-film meter (9) before the gas released into the atmosphere. The gas absorption rate was calculated as the difference between inflow and outflow rate. In the experiments, inflow was between 4.7×10^{-4} mol/s and 11×10^{-4} mol/s.

Physical properties

Interpretation and correlations of the mass transfer data obtained require knowledge of the densities, ρ (kg/m^3), viscosities, μ (kg/m·s), and surface tensions, σ (N/m), of the liquid phases, as well as the solubilities and diffusivities of the gas in absorption phases.

The densities and viscosities of the sodium carbonate-bicarbonate buffer solutions, with surfacetant and sodium arsenite, were measured at 298.15 K using a Gay-Lussac type pycnometer and an Ubbelohde viscometer, respectively. However, neither of these properties differed significantly from the values for the buffer solutions: ρ=1042 kg/m^3 and μ=1.29×10^{-3} kg/m·s.

The surface tension was determined by a stalagmometer. The surface tensions of the solutions at 298.15 K are listed in Table 4.

The diffusivity of CO_2 in buffer solution of Na_2CO_3-$NaHCO_3$, D_d, can be estimated from the diffusivity of CO_2 in pure water, D_w (m^2/s), by the following equation (Hikita *et al.*, 1976; Vázquez *et al.*, 2000; Cents *et al.*, 2001):

$$D_d / D_W = 1 - \sum_{i=1}^{2} (\xi_i C_i) \qquad (16)$$

where C_i is concentration of electrolyte i (Na_2CO_3 or $NaHCO_3$) in buffer solution (mol/L); and ξ_i is function of temperature for electrolyte i which can be estimated by:

$$\xi_i = 0.030 + 0.550\omega_i \qquad (17)$$

the coefficient, ω_i, can be estimated from the viscosity of pure water and solution of electrolyte i as:

$$\mu_{\mathrm{w}} = \mu_i(1 + \omega_i C_i) \qquad (18)$$

where μ_{w} and μ_i are the viscosity of pure water and solution of electrolyte i, respectively.

The diffusivities of CO_2 can then be calculated at various temperatures using D_{W} (Perry and Green, 1997) as listed in Table 2.

The solubilities of CO_2 in buffer solutions with DBS and/or sodium arsenite, due to the electrolytic nature, were calculated from Eq.(19) proposed by Danckwerts and Gillham (Hikita *et al.*, 1976; Cents *et al.*, 2001) for solutions containing more than one electrolyte:

$$\lg\left(\frac{C^{\mathrm{e}}}{C_{\mathrm{d}}^{\mathrm{e}}}\right) = -\sum_{i=1}^{2}(K_{si}I_i) \qquad (19)$$

where I_i and K_{si} (L/mol) are the ionic strength and the salting out parameter for electrolyte i (Na_2CO_3 or $NaHCO_3$), respectively; and C^{e} is the solubility of CO_2 in pure water (mol/L).

In Table 3, the values of I_i were calculated from the experiments, K_{si} was taken from Danckwerts (1970), and C^{e} was taken from Perry and Green (1997).

It was proved that the addition of sodium arsenite affected neither the diffusivity nor the solubility of CO_2 due to its low concentration.

RESULTS AND DISCUSSION

The absorption rate of CO_2, n (mol/L), depends on the superficial gas velocity, u_{G} (m/s), and the concentration of catalyst and surfactant, as Fig.2 showing that n, the plateau value of the absorption curve, increases with increasing concentration of catalyst, and decreases with increasing concentration of DBS.

When the absorption rate of CO_2 was evaluated, the specific interfacial area, a, and the individual mass transfer coefficient, k_{L}, were determined by Danckwerts method. In accordance with this method, Fig.3 shows N^2 plotted versus k_1 for one of the superficial gas velocities and for different temperatures, whereas Fig.4 shows N^2 plotted versus k_1

for one of the temperatures and for different superficial gas velocities; Fig.5 shows N^2 plotted versus k_1 for one of the temperatures and for different surface tensions. The Danckwerts plots of Figs. 3, 4, and 5 show excellent linearity, implying that this method can be used for determining a and k_{L} simultaneously, whose values are listed in Table 4.

Table 4 shows that the specific interfacial area, individual mass transfer coefficient and volumetric mass transfer coefficient apparently depend on the temperature, superficial gas velocity, and aqueous surface tension.

a decreases, but k_{L} and $k_{\mathrm{L}}a$ increase with increasing temperature. When temperature increased, the decreased surface tension of the solution caused a to decrease, whereas the increased molecular random movement caused the k_{L} to increase.

When the gas flow rate or superficial gas velocity decreased, the gas hold-up decreased, which caused a, k_{L}, and $k_{\mathrm{L}}a$ to decline.

a, k_{L}, and $k_{\mathrm{L}}a$ decreased with increasing concentration of DBS, or decreased with decreasing of surface tension. This reduction may be attributed to the effect of the surface-active agent, which can reduce the interfacial movement when it occupies part of the surface of the bubble. Furthermore, the surface concentration of the surfactant increases with the surfactant concentration in the liquid bulk (Vázquez *et al.*, 1997; Joshi, 2001).

Using non-linear least square regression to analyze the experimental results in Table 4, the specific interfacial area, individual mass transfer coefficient, and volumetric mass transfer coefficient can be correlated with temperature, superficial gas velocity, and surface tension as follows:

$$\ln(k_{\mathrm{L}}) = 4.13 + 0.797\ \ln(\sigma) + 0.411\ \ln(u_{\mathrm{G}}) - \frac{2.59 \times 10^3}{T}$$
$$r = 0.993 \qquad (20)$$

$$\ln(a) = 7.30 - 1.30 \times 10^{-3}\ln(\sigma) + 0.634\ \ln(u_{\mathrm{G}}) + \frac{292}{T}$$
$$r = 0.972 \qquad (21)$$

$$\ln(k_{\mathrm{L}}a) = 11.43 + 0.796\ \ln(\sigma) + 1.045\ \ln(u_{\mathrm{G}}) - \frac{2.30 \times 10^3}{T}$$
$$r = 0.982 \qquad (22)$$
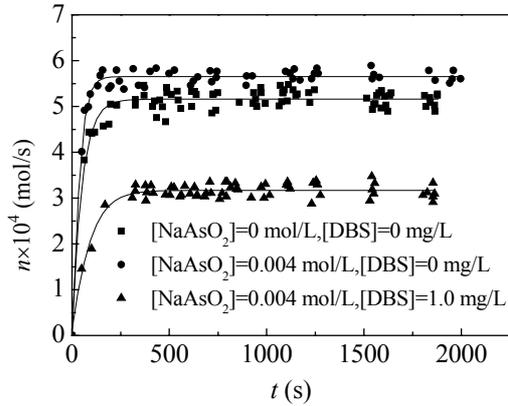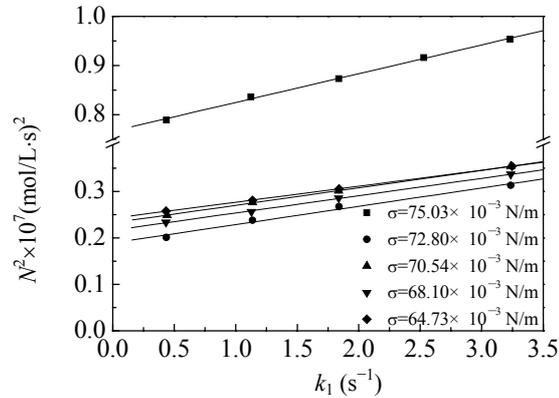
Fig.2 Time-dependence of *n* for different concentrations of NaAsO₂ and DBS. *T*= 298.15 K
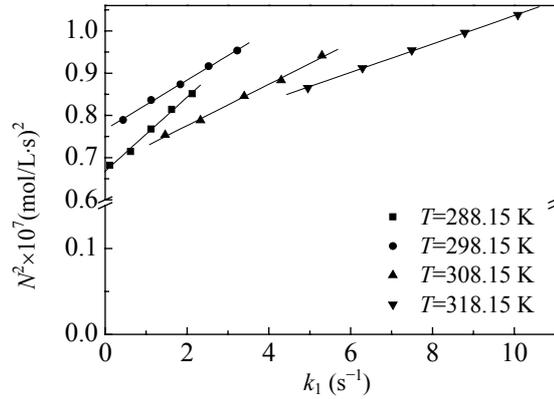
Fig.3   Danckwerts   plots   when   temperatures   varied. [DBS]=0 mg/L, *u*_G=0.0031 m/s
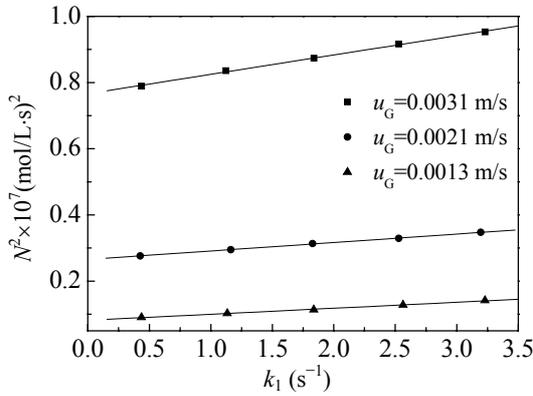
Fig.4   Danckwerts plots when superficial gas velocities varied. [DBS]=0 mg/L, *T*= 298.15 K

Fig.5 Danckwerts plots when surface tensions varied. *u*_G=0.0031 m/s , *T*= 298.15 K

The calculated values from Eqs.(20)–(22) are listed in Table 4. Considering the values of the specific interfacial area, individual mass transfer coefficient, and volumetric mass transfer coefficient, the deviations between the experimental results and the calculations from Eqs.(20)–(22) were actually always lower than 10%, which demonstrated that the correlation equations fitted the experimental results well.

CONCLUSIONS

In this study, the presence of the surfactant induced reduction of the specific interfacial area and the individual mass transfer coefficient. Both

specific interfacial area and individual mass transfer coefficient increased with increasing superficial gas velocity. The specific interfacial area decreased, whereas the individual mass transfer coefficient increased with increasing temperature.

The specific interfacial area, individual mass transfer coefficient, and volumetric mass transfer coefficient were well correlated with temperature, superficial gas velocity, and surface tension with a deviation within 10% using non-linear least square regression analysis.

References

Cents, A.H.G., Brilman, D.W.F., Versteeg, G.F., 2001. Gas absorption in an agitated gas-liquid-liquid system. *Chem. Eng. Sci.*, **56**:1075-1083.

Danckwerts, P.V., 1970. Gas-Liquid Reactions. McGraw-Hill, New York, p.35-245.

Hikita, H., Asai, S., Takatsu, T., 1976. Absorption of carbon dioxide into aqueous sodium hydroxide and sodium carbonate solutions. *Chem. Eng. J.*, **11**:131-141.

Joshi, J.B., 2001. Computational flow modeling and design of bubble column reactors. *Chem. Eng. Sci.*, **56**:5893-5933.

Lorenzen, L., Kleingeld, A.W., 2000. New generation leaching reactors for effective mass transfer in mineral processing operations. *Minerals Engineering*, **13** (10-11):1107-1115.

Lye, G.J., Stuckey, D.C., 2001. Extraction of erythromycin-A using colloidal liquid aphrons: Part II. Mass transfer kinetics. *Chem. Eng. Sci.*, **56**:97-108.

Mitsuharu, I., Hiroki, U., Toshifumi, I., 2001. Mass transfer characteristics in gas bubble dispersed phase generated by plunging jet containing small solute bubbles. *Chem. Eng. Sci.*, **56**:6225-6231.

Perry, R.H., Green, D.W., 1997. Perry's Chemical Engineers' Handbook, 7th Edition. McGraw-Hill, New York, p.2-330.

Vázquez, G., Cancela, M.A., Varela, R., Alvarez, E., Navaza, J.M., 1997. Influence of surfactants on absorption of CO_2 in a stirred tank with and without bubbling. *Chem. Eng. J.*, **67**:131-137.

Vázquez, G., Cancela, M.A., Riverol, C., Alvarez, E., Navaza, J.M., 2000. Application of the Danckwerts method in a bubble column: Effects of surfactants on mass transfer coefficient and interfacial area. *Chem. Eng. J.*, **78**:13-19.

Wu, Z.C., Zhou, M.H., Huang, Z.W., Wang, D.H., 2002. Electrocatalysis method for wastewater treatment using a novel *beta*-lead dioxide anode. *Journal of Zhejiang University SCIENCE*, **3**(2):194-198.

Yang, Y.P., Wu, X.Y., Xu, X.H., Wang, D.H., 2001. Treatment of dyeing wastewater by photo-assisted Fenton system. *Journal of Chemical Engineering of Chinese Universities*, **15**(3):242-247 (in Chinese).